

EXPLORING THE RHEOLOGICAL PROPERTIES OF WATERBORNE POLYURETHANE/CARBON QUANTUM DOTS NANOCOMPOSITES WITH PHOTOACTIVE CHARACTERISTICS

Lucas Dall Agnol^{1*}, Fernanda T. G. Dias² and Otávio Bianchi^{1,3}

1 – Postgraduate Program in Materials Science and Engineering (PGMAT), University of Caxias do Sul (UCS), Caxias do Sul, RS, Brazil

agnol.lucasdall@gmail.com and otavio.bianchi@gmail.com

2 – Department of Organic Chemistry, Institute of Chemistry, Federal University of Rio Grande do Sul (UFRGS), Porto Alegre, RS, Brazil

3 – Department of Materials Engineering (DEMAT), Federal University of Rio Grande do Sul (UFRGS), Porto Alegre, RS, Brazil

Abstract: Incorporating carbon quantum dots (CQDs) into waterborne polyurethane (WPU) can significantly impact its rheological behavior, which is crucial for optimizing its performance in applications such as surface coating. This study investigated the effect of adding 1.0 wt.% of CQDs on the rheological behavior of WPU. Oscillatory shear measurements were conducted at different temperatures (110–180 °C), and the resulting master curves revealed a shear-thinning behavior for the materials. Furthermore, both the nanocomposite containing 1.0 wt.% CQDs (WPU1) and the neat polymer (WPU0) exhibited practically identical flow activation energy (~ 80 kJ/mol), despite the higher molar mass of WPU1 due to CQDs' polyfunctionality. The slight reduction in the system's viscosity due to CQDs' presence can be attributed to the sliding effect of small particles (<10 nm) on polymer nanocomposites, seeming not to compromise its application as a functional coating.

Keywords: waterborne polyurethane; carbon quantum dots; photoactive coating; viscosity; flow activation energy.

Introduction

Photoluminescent materials have attracted attention for sensing due to their distinct advantages over solution-based probes, including excellent stability, ease of transport, storage, recycling, non-invasive nature, and tunable shape and size. The potential application of CQDs in developing these photoluminescent materials has already been demonstrated [1]. These materials' surface hydroxyl and carboxyl groups provide excellent solubility in water and organic solvents but hinder their deposition as thin films by conventional methods. Moreover, in environments where they are insoluble, these nanostructures lose their photoactivity in the solid-state [2]. Using a polymer matrix as support can facilitate the application of CQDs and prevent their photoluminescence loss, also providing mechanical resistance and catalytic stability to the final material. In this context, WPU emerges as an option for CQDs support due to its exceptional mechanical, chemical, and adhesion properties and low emission of organic volatiles [3]. Also, the excellent transparency of polyurethane makes it an ideal matrix for producing suitable fluorescent materials [1]. WPU is soluble in water, contributing to CQDs distribution in the matrix and preserving their photoluminescence activity. During synthesis, the polyurethane chains can be chemically linked at the surface of the embedded CQDs to form a slightly crosslinked network structure, improving nanocomposite properties [1]. It is known that the presence of CQDs can influence the rheological behavior of polymer nanocomposite. At low concentrations, the CQDs may not significantly affect WPU rheology. At higher concentrations, however, small particles can form aggregates that alter the viscosity of polymer systems. Most works and patents on WPU/CQDs mainly report the industrial applications of these systems [4, 5], without

deeply investigating the relationship between structure, rheological behavior, and coating performance of such materials under their typical service conditions [1].

Thus, the current work aims to investigate the effect of incorporating only 1.0 wt.% of CQDs on the rheological behavior of the WPU. The film's rheological investigation involved small-amplitude oscillatory shear measurements at different temperatures, determination of flux activation energy (E_a), and generation of master curves capable of predicting material's performance under particular conditions. Indeed, this information will contribute to optimizing processing conditions and designing WPU/CQDs nanocomposites with tailored properties that could be applied as functional coatings. We need to understand how the addition of CQDs can affect the nanocomposite's flow properties.

Experimental

Synthesis of CQDs: The CQDs were produced by microwave-assisted pyrolysis of an aqueous solution of citric acid (CA; 98.5% purity, Sigma Aldrich) and ethylenediamine (EDA; $\geq 99.5\%$ purity, Sigma Aldrich) (1:1 molar ratio) according to [1]. Briefly, the mixture was first ultrasonicated for 2 min (20 MHz) and then irradiated for 6 min in a domestic microwave oven (650 W). The resulting red-brown solid was purified by dialysis in ultrapure water (MWCO membrane of 1000 Da) for 3 days. Then, the CQDs were vacuum-dried at 65 °C (reaction yield was about 78 %).

Synthesis of WPU/CQDs nanocomposites: The WPU/CQDs dispersion was initially prepared by an oil heating flask reaction of hexamethylene diisocyanate (HDI, $\geq 99\%$ purity, Sigma Aldrich) and polycarbonate diol (PCD, 2000 g/mol; UBE Corporation Europe) for 4 h at 80 °C under nitrogen atmosphere. Then, 2,2-bis(hydroxymethyl)propionic acid (DMPA, 98% purity, Sigma Aldrich) was incorporated into the –NCO-terminated prepolymer by reaction at 80 °C for 2 h. Acetone was added to control the reaction medium viscosity. Subsequently, the reaction temperature was reduced to 45 °C, and triethylamine (TEA, $\geq 99.5\%$ purity, Sigma Aldrich) was added (~45 min) to neutralize the carboxyl groups in the prepolymer. Finally, the prepolymer was dispersed in aqueous solutions containing 1.0 wt.% CQDs under vigorous stirring (1100 rpm) for 30 min. The stoichiometric ratio of HDI/PCD/DMPA/TEA was 3:1:1:1.2. The residual solvents were removed by distillation under reduced pressure (60 °C for 1 h). The dispersion's solids content was about 30% by weight. For characterization, WPU/CQDs films were prepared on a Teflon substrate by dispersions drying in an oven. Two samples were prepared, one without CQDs, named WPU0 and the other with 1.0 wt.% CQDs, named WPU1. This CQDs content was chosen based on the best results of [1].

Chemical structure and photoluminescence: The chemical structure, thermal and mechanical properties and photoluminescence behavior of WPU/CQDs nanocomposite was shown and discussed in detail in Dall Agnol *et al.* [1]. Here, only the main findings will be punctuated, whose information is relevant to understanding the rheological data of these materials.

Rheological behavior: All rheological measurements were performed on the materials films obtained after water evaporation (0.5 mm thickness) in an Anton Paar MCR 101 rheometer (parallel plates geometry, 25 mm diameter, 0.5 mm gap) under a nitrogen atmosphere. Small-amplitude oscillatory shear measurements were evaluated at 100–180 °C, using angular frequency sweep mode (0.1–500 rad/s) and strain amplitude of 1% (linear viscoelastic regime). The zero-shear viscosity (η_0) was calculated by fitting the complex viscosity (η^*) vs. angular frequency (ω) data to the Cross model [1]. After fitting the η^* vs. ω experimental data, the flux activation energy was calculated using the Arrhenius equation (Equation 1). This equation is a phenomenological model that relates the reaction rate's temperature dependence to the reaction's activation energy (E_a). It can be expressed as:

$$\eta_0^* = A \cdot e^{-\frac{E_a}{RT}} \quad (1)$$

where η_0^* is the zero shear/frequency viscosity obtained by Cross model fit, A is the pre-exponential factor, E_a is the activation energy, R is the gas constant, T is the absolute temperature, and e is the exponential function. By taking the logarithm of the expression and plotting $\ln(\eta_0^*)$ vs. $1/T$, the E_a can be determined from the slope of the resulting straight line. In this case, the Arrhenius equation was

used to calculate the flux activation energy, which measures the energy required for the flow of the molten WPU/CQDs nanocomposite. From carrying out the rheological experiments at various temperatures, it was possible to generate a set of master curves based on the relationship between experimental data and a particular reference temperature. Master curves allow the prediction of material behavior under temperatures different from those tested, enabling a better understanding of material performance in a variety of conditions:

$$\eta^*(\omega, T, p) = \eta_0^{**} [1 + A_1(\eta_0^* \omega)^\alpha + A_2(\eta_0^* \omega)^{2\alpha}]^{-1} \quad (2)$$

where, A_1 , A_2 and α are fitted parameters. In this case η_0^{**} is the value of the zero shear/frequency viscosity obtained by the master curve.

Results and Discussion

The CQDs as-synthesized presented carboxyl, hydroxyl, and amino surface groups capable of interacting strongly with the flexible and rigid segments of WPU, which has been characterized in [1, 2]. This work investigated the effect of incorporating CQDs on the molten state rheological properties of WPU. Fig. 1 shows the dependence of η^* as a function of ω for WPU0 and WPU1. Complex viscosity (η^*) decreases with the addition of CQDs, especially at low frequencies, which may be related to the lubrication caused by nanoparticles [6]. Table 1 shows the rheological parameters obtained by fitting Cross's equation to the experimental data. The viscoelastic behavior of WPU0 and WPU1 was pseudoplastic, as evidenced by a decrease in viscosity with increasing oscillation frequency. The Cross-model adjustments yielded correlation coefficients above 0.9. The incorporation of CQDs caused a reduction in the λ values. A high λ value indicates that a relatively high oscillatory shear is required to cause structural failure. In contrast, a low λ value corresponds to a weaker structure that can be disrupted at lower shear rates (frequencies). Consequently, the Newtonian plateau transition occurs at lower frequencies due to the increased viscous dissipation induced by CQDs.

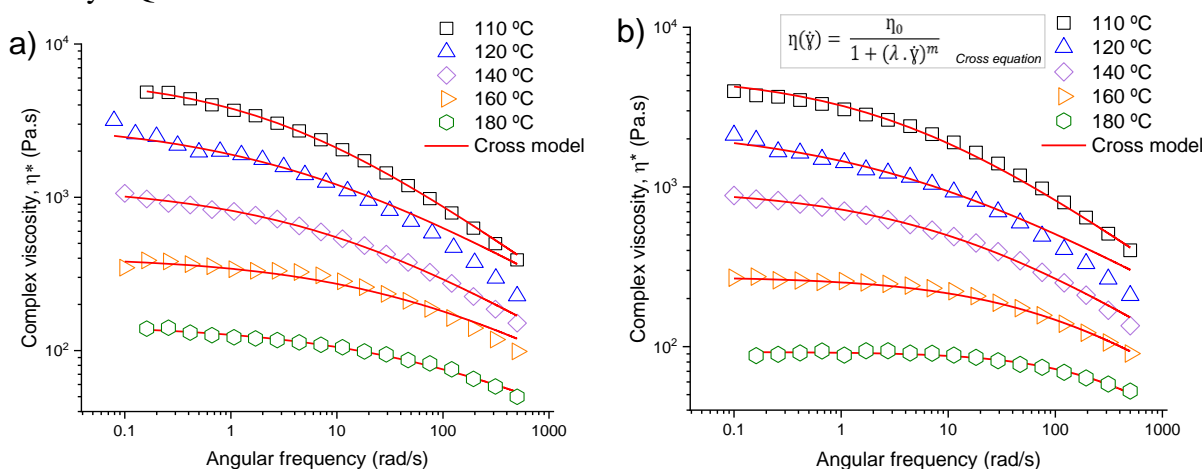


Figure 1 – Dependence of complex viscosity (η^*) as a function of angular frequency (ω) for (a) WPU0 and (b) WPU1

Table 1 – Rheological parameters obtained by fitting the Cross equation for WPU0 and WPU1

Sample	T (°C)	η_0^* (Pa.s)	λ (s)	m	R ²	Sample	T (°C)	η_0^* (Pa.s)	λ (s)	m	R ²
WPU0	110	6120	0.370	0.49	0.9988	WPU1	110	4491	0.300	0.48	0.9992
	120	3661	0.300	0.40	0.9799		120	2630	0.300	0.38	0.9788
	140	1178	0.140	0.42	0.9955		140	975	0.090	0.43	0.9982
	160	411	0.018	0.40	0.9888		160	271	0.007	0.50	0.9906
	180	148	0.009	0.37	0.9886		180	93	0.001	0.66	0.9648

η_0^* : complex viscosity at zero frequency; λ : time-dependent parameter associated with the transition from the Newtonian *plateau*; m: dimensionless ($m \rightarrow 1$ = pseudoplastic behavior, $m \rightarrow 0$ = Newtonian fluid behavior); R²: correlation coefficient.

As expected, the η_0^* values decreased with increasing temperature for both WPU0 and WPU1 systems. However, the WPU1 system exhibited lower viscosities than neat WPU0, despite having a higher molar mass according to SEC data (M_n , WPU0 = 26,476 g/mol and WPU1 = 27,066 g/mol, polydispersity ~ 2 for both [1]). This could be attributed to the sliding effect caused by the CQD particles, which can favor the polymer chains' flow and reduce the system's overall viscosity. The flux activation energy was estimated using Eq. 1 (Fig. 2).

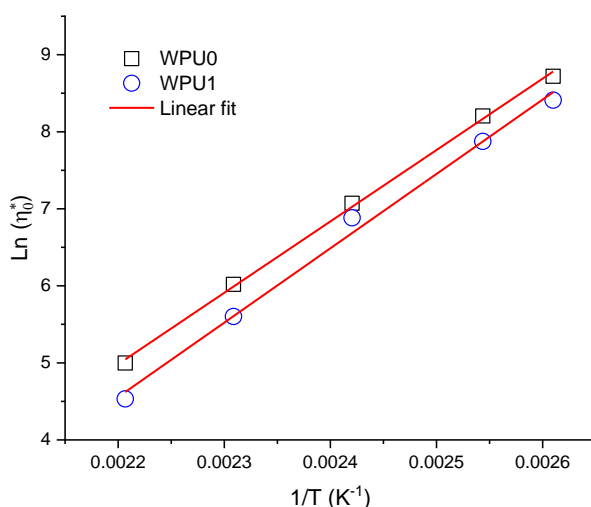


Figure 2 – Linear fit slope of $\ln(\eta_0^*)$ vs. $1/T$ data for E_a determination

The WPU0 exhibited a flux E_a of 77 kJ/mol, whereas the addition of CQDs led to a slightly higher value of 80 kJ/mol for WPU1. This result was unexpected, considering that SEC analyses showed an increase in the molar mass of the system with CQDs. However, the polyfunctionality of the CQDs had a negligible effect on the flow activation condition. This phenomenon could be attributed to the small size of the particles, which could cause a reduction in viscosity as previously reported by [1, 6]. In conclusion, CQDs did not significantly affect the flux E_a , despite the larger molar mass of WPU1. Fig. 3 (a) and (b) schematically illustrate the master curve derived from η^* data that depends on oscillatory shear (WPU0 and WPU1). To obtain a dimensionless number, $\log \eta/\eta_0$, viscosity is divided by viscosity at zero shear or frequency. Parameter $\log \eta/\eta_0$ approaches zero when the viscosity is shear-independent (Newtonian plateau) and becomes negative in the shear-thinning region.

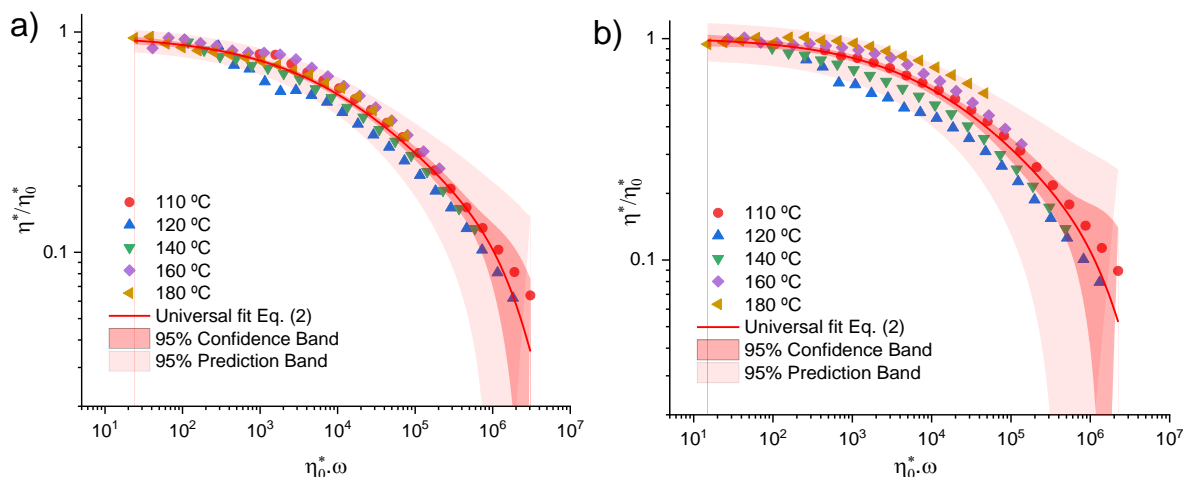


Figure 3 – Master curve from η^* data for a) WPU0 and b) WPU1

Regarding the master curve adjustment, both samples showed a smaller dispersion of experimental points at lower frequencies. The parameters of Eq. 2 were adjusted with R^2 greater than 0.9 for both samples. The following parameters were obtained for WPU0 ($A_1 = 0.013$, $A_2 = 3.54 \times 10^{-12}$, $\alpha = 0.45$, and $\eta_0 = 0.96$) and WPU1 ($A_1 = 0.008$, $A_2 = 3.58 \times 10^{-12}$, $\alpha = 0.47$, and $\eta_0 = 1.01$). Assuming that $\alpha =$

$1-n$, where n is the power index, it can be inferred that both systems exhibit a shear-thinning behavior. However, the sliding effect caused by the small particles alters the transition region of the Newtonian plateau for the polymeric chain [6].

Conclusions

Here, we explored the effect of photoluminescent CQDs on the rheological behavior of a waterborne polyurethane nanocomposite synthesized by *in situ* polymerization. The WPU1 nanocomposite (containing 1 wt.% CQDs) and the neat polymer showed the same flux activation energy (E_a). Furthermore, a master viscosity function was obtained, indicating a shear-thinning behavior for WPU0 and WPU1. Interestingly, the addition of small particles such as CQDs (<10 nm [1]) leads to a reduction in the polymer nanocomposite viscosity despite the increase detected in its molar mass. Other studies also observed a viscosity reduction of the polymer matrix by incorporating C-dots [7, 8]. Some mechanisms for this nanocomposite viscosity reduction were pointed out in these works, such as the nanoparticles' radius of gyration and polymer molar mass, polymer degradation induced by nanoparticles, adsorption of polymers on nanoparticles' surface, free volume effect and particle agglomeration, changes in the entanglement density of polymer chains, and the sliding effect caused by nanoparticles with favored chains' flow, which is the mechanism suggested by the authors for the WPU/CQDs system. From the results, the incorporation of only 1.0 wt.% CQDs caused a slight change in the polymer matrix rheology, both in viscosity and flow activation energy, indicating that this nanoparticle content would not affect the WPU/CQDs nanocomposite performance as a functional coating. Besides the promising luminescent characteristics of this nanocomposite, it was essential to investigate its rheological behavior for applications under high temperatures or thermal cycles conditions.

Acknowledgements

The authors acknowledge Brazilian Agency Coordenação de Aperfeiçoamento de Pessoal de Nível Superior (CAPES, Brazil) and Fundação de Amparo à Pesquisa do Estado do Rio Grande do Sul (FAPERGS, Brazil; grants: 19/2551-0001843-6).

References

1. L. Dall Agnol, F.T.G. Dias; O. Bianchi, *Prog. Org. Coat.* 2023, 179. <https://doi.org/10.1016/j.porgcoat.2023.107492>.
2. Y. Zhang; X. Liu; Y. Fan; X. Guo; L. Zhou; Y. Lv; J. Lin, *Nanoscale* 2016, 8, 15281. <https://doi.org/10.1039/C6NR03125K>.
3. L. Dall Agnol; F.T.G. Dias; H.L. Ornaghi; M. Sangermano; O. Bianchi, *Prog. Org. Coat.* 2021, 154. <https://doi.org/10.1016/j.porgcoat.2021.106156>
4. R. Duarah; Y.P. Singh; P. Gupta; B.B. Mandal; N. Karak, *Biofabrication* 2016, 8, 045013. <https://doi.org/10.1088/1758-5090/8/4/045013>.
5. M. Kovacova; Z.M. Markovic; P. Humpolicek, *et al.*, *ACS Biomater. Sci. Eng.* 2018, 4, 3983. <https://doi.org/10.1021/acsbiomaterials.8b00582>.
6. O. Bianchi; H.L. Ornaghi; J.N. Martins; C. Dal Castel; L.B. Canto, *Polym. Eng. Sci.* 2020, 60, 2272. <https://doi.org/10.1002/pen.25469>.
7. M.A. Haruna; Z. Hu; H. Gao; J. Gardy; S.M. Magami; D. Wen, *Fuel* 2019, 248, 205. <https://doi.org/10.1016/j.fuel.2019.03.039>.
8. G. Yao; J. Zhao; M.A. Haruna; D. Wen, *RSC advances* 2021, 11, 26037. <https://doi.org/10.1039/D1RA03935K>.